Quasibound states of Schrödinger and Dirac electrons in a magnetic quantum dot

M. Ramezani Masir,[1,*] A. Matulis,[1,2,†] and F. M. Peeters[1,3,‡]
[1]*Departement Fysica, Universiteit Antwerpen, Groenenborgerlaan 171, B-2020 Antwerpen, Belgium*
[2]*Semiconductor Physics Institute, Goštauto 11, LT-01108 Vilnius, Lithuania*
[3]*Departamento de Física, Universidade Federal do Ceará, Caixa Postal 6030, Campus do Pici, 60455-760 Fortaleza, Ceará, Brazil*
(Received 26 January 2009; published 30 April 2009)

The properties of a two-dimensional electron are investigated in the presence of a circular step magnetic-field profile. Both electrons with parabolic dispersion as well as Dirac electrons with linear dispersion are studied. We found that in such a magnetic quantum dot no electrons can be confined. Nevertheless close to the Landau levels quasibound states can exist with a rather long lifetime.

DOI: 10.1103/PhysRevB.79.155451 PACS number(s): 73.63.Kv, 73.43.Cd, 81.05.Uw

I. INTRODUCTION

During the last five years, graphene (a single layer of carbon atoms) has become a very active field of research in nanophysics.[1,2] It is expected that this material will serve as a base for new electronic and optoelectric devices. One of the most challenging tasks is to learn how to control the electron behavior using electric fields in this two-dimensional (2D) layer. This task is made complicated by the so-called Klein effect according to which Dirac electrons in graphene can tunnel through any electric barrier.[3] As a consequence in electrically created quantum dots there are no bound states but only quasibound states, or so-called resonances[4–6] which, however, under certain conditions can have a long lifetime.

An alternative approach to control the motion of electrons is to use nonhomogeneous magnetic fields which can be created, e.g., through the deposit of nanostructured ferromagnets.[7–9] Recently it was shown that nonhomogeneous magnetic structures are able to confine Dirac electrons in graphene.[10–19] However, up to now semi-infinite (homogeneous in one direction) structures were considered, which makes the analysis more simple because the problem is reduced into a one-dimensional one.

In this paper we consider a finite-size magnetic structure where the magnetic field is nonzero only in a finite region of space. Namely, we consider a model homogeneous magnetic field that is nonzero in a circle that we call the magnetic dot. This situation is the inverse of the one considered in Ref. 11 where a magnetic antidot was considered, as in Ref. 9 for the case of normal electrons, where the magnetic field is zero in a circular region and nonzero outside this region. Such a model system can be realized by having a magnetic vortex piercing the graphene layer or by overlaying graphene with type I superconductor with a circular hole placed in the perpendicular magnetic field. In order to reveal the peculiarities of the behavior of Dirac electrons in such magnetic dot we compare the result with those for standard electrons with parabolic dispersion law.

We show that it is impossible to confine 2D electrons in a magnetic dot in contrast to semi-infinite magnetic structures neither in the case of graphene nor in the case of the standard electron, and consequently, all Landau levels convert themselves into unbound states. Nevertheless, long living quasibound states can be present. We studied them using the local density of states technique applied previously for the investigation of electrically confined electrons.[5]

The paper is organized as follows. In Sec. II the model of a magnetic dot for a standard electron is considered. The problem is formulated in Sec. II A, the local density of states technique is presented in Sec. II B, the results are discussed in Sec. II C, while in Sec. II D the complex energy eigenvalues of the problem are described. In the corresponding subsections of Sec. III the problem of the Dirac electron in a magnetic dot is presented. Our conclusions are given in Sec. IV.

II. ELECTRON WITH PARABOLIC ENERGY DISPERSION

We assume that a homogeneous magnetic field $\mathbf{B}_0$ is present in a circular area of radius r_0, while there is no magnetic field outside it, namely, $\mathbf{B}_0(\mathbf{r})=\mathbf{e}_z B_0\Theta(r_0-r)$. The behavior of the electron is described by the stationary Schrödinger equation

$$\{H-E\}\Psi(\mathbf{r})=0, \tag{1}$$

with the Hamiltonian

$$H=-\frac{1}{2}(\nabla+i\mathbf{A})^2. \tag{2}$$

Because of the cylindric symmetry of the problem we choose the symmetric gauge for the vector potential defining its single azimuthal component as

$$A_\varphi(r)\equiv=\frac{1}{2}\begin{cases} r, & r<r_0 \\ r_0^2/r, & r_0<r. \end{cases} \tag{3}$$

This azimuthal component is shown in Fig. 1 together with the magnetic-field profile.

In order to simplify the notations we use dimensionless variables, based on the magnetic-field strength value B_0. Thus, the magnetic field $B(\mathbf{r})$ is measured in B_0 units; all distances are measured in the unit of magnetic length $l_B=\sqrt{c\hbar/eB_0}$, energy and potential in $\hbar\omega_c$ ($\omega_c=eB_0/mc$), and vector potential in $B_0 l_B$ units. In the case of electron moving at a GaAs/AlGaAs interface ($m^*=0.067$) and magnetic field

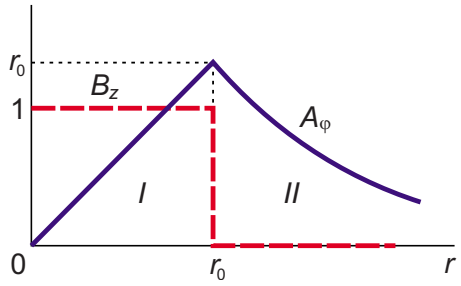

FIG. 1. (Color online) Azimuthal vector potential component A_φ (blue solid curve) and perpendicular magnetic field B_z (red dashed curve) as functions of the radial coordinate.

of 1 T the unit of length is l_B=250 nm, and the energy unit is 20 meV.

A. Solution of eigenvalue problem

The Schrödinger Eq. (1) in cylindric coordinates reads

$$\left\{\frac{1}{r}\frac{\partial}{\partial r}r\frac{\partial}{\partial r}+\frac{1}{r^2}\frac{\partial^2}{\partial\varphi^2}+\frac{iA_\varphi}{r}\frac{\partial}{\partial\varphi}-A_\varphi^2+2E\right\}\Psi=0. \quad (4)$$

Substituting the wave function

$$\Psi\equiv\Psi(r,\varphi)=e^{im\varphi}\psi(r), \quad (5)$$

we arrive at the radial equations

$$\left\{\frac{1}{r}\frac{d}{dr}r\frac{d}{dr}-\left(\frac{m}{r}+\frac{r}{2}\right)^2+2E\right\}\psi_{\rm I}(r)=0, \quad (6a)$$

$$\left\{\frac{1}{r}\frac{d}{dr}r\frac{d}{dr}-\frac{(m+r_0^2/2)^2}{r^2}+2E\right\}\psi_{\rm II}(r)=0, \quad (6b)$$

which have to be solved inside the dot (region I) and outside it (region II). The boundary conditions (the continuity of the wave function and its radial derivative) have to be satisfied at the dot border ($r=r_0$).

The regular solution inside the dot can be expressed via the confluent hypergeometric function [Kummer function $M(a|c|z)$]:

$$\psi_{\rm I}(r)=Af(r)=Ar^{|m|}e^{-r^2/4}\times M[(|m|+m)/2+1/2-E||m|+1|r^2/2], \quad (7)$$

while the solution outside it is composed of two Bessel functions

$$\psi_{\rm II}(r)=BJ_\nu(kr)+CY_\nu(kr), \quad (8)$$

where $k=\sqrt{2E}$ is the momentum of the free electron (measured in l_B^{-1} units), and $\nu=m+r_0^2/2$. Note both functions (J_ν and Y_ν) suit us, as they vanish in the limit $r\to\infty$.

Thus, we have three constants A, B, and C. They cannot be defined from the above-mentioned two boundary conditions. That is why we have to conclude that there are no bound states, and consequently, a magnetic field in a finite region of the 2D plane cannot confine the electron. However,

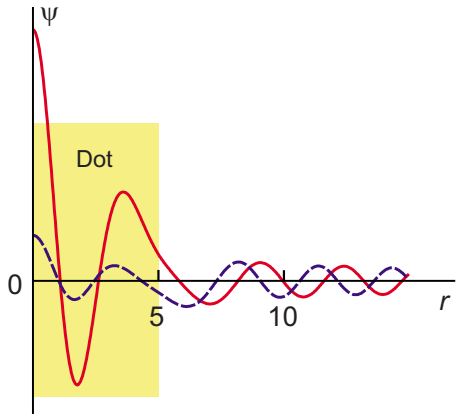

FIG. 2. (Color online) The wave functions for m=0, r_0=5: E=2.5—red solid curve, and E=2.8—dashed blue curve. The magnetic dot region is indicated by shadowed rectangle.

quasibound states can be expected when the electron energy in the dot is close to the Landau levels with energy

$$E_{n,m}=n+\frac{|m|+m+1}{2} \quad (9)$$

(here $n=0,1,\cdots$ and $m=0,\pm1,\cdots$) defined in the case of homogeneous magnetic field. Confirmation of this statement follows from Fig. 2, where the electron wave functions for two different energies are shown.

We see that in the case of E=2.5 (red solid curve) which corresponds to the Landau level with n=2 and m=0 the wave function is large in the dot region (shown in Fig. 2 by shadowed yellow rectangle), while for the case of energy E=2.8, which does not coincide with any Landau level energy, it does not have any appreciable large value inside the dot, and actually does not differ much from the wave function for a free electron calculated in cylindric coordinates.

B. Local density of states

Next we will look for possible long living quasistationary states in the magnetic dot. In principle such quasibound (or quasistationary) states have to be described by the solution of the time-dependent Schrödinger equation which is much more complicated as compared with the standard eigenvalue problem. There are, however, several alternative approaches which enable us to investigate properties of quasibound states by stationary means. We follow the method presented in detail in Ref. 5 and calculate the local density of states. The basic idea is to confine the electron in a large region of finite radius R, where its wave function obeys the zero boundary condition at the border ($r=R$) and treat the problem as a stationary one. A measurement that probes quantum dot properties, say, measuring of the tunneling current directed perpendicular to the dot with STM, or power absorption in near-field infrared spectroscopy, has to depend on the averaged value of the electron wave function in the dot. Therefore we introduce the integral

$$\mathcal{I}(E) = 2\pi \int_0^\infty r dr F(r) |\Psi(r)|^2, \tag{10}$$

which depends on the electron wave function, and actually is proportional to the so-called *local density of states*. The aperture function $F(r)$ characterizes the interaction of the electron with the measuring probe.

This integral is sensitive to the probability to find the electron in the dot, and in the case of a quasibound state it will exhibit a peak corresponding to the energy of this state. The width of the peak is related to the inverse of the lifetime of this quasistationary state.

For the sake of determinacy we use the aperture function of a Gaussian,

$$F(r) = b r_0^2 e^{-b r^2}, \quad b = r_0^{-2} \ln 10, \tag{11}$$

which corresponds to the probability to find the electron in the dot area πr_0^2. In the case of larger b value instead of the local density of states we obtain the squared wave function value in the center of the dot, while in the case of smaller b value the peculiarities of the dot are washed out.

The solution of the Schrödinger Eq. (6) given by Eqs. (7) and (8) has to satisfy the following boundary conditions:

$$\psi_{\mathrm{I}}(r_0) = \psi_{\mathrm{II}}(r_0), \tag{12a}$$

$$\psi_{\mathrm{I},r}(r_0) = \psi_{\mathrm{II},r}(r_0), \tag{12b}$$

$$\psi_{\mathrm{II}}(R) = 0, \tag{12c}$$

which converts our problem into an eigenvalue problem. Here and further the subscript $_r$ means the derivative over r.

At the end, we are interested in the limiting case $R \to \infty$. Therefore, in the last of Eq. (12) we replace the Bessel functions by their asymptotic, namely, we have

$$B \cos(kR - \varphi_m) + C \sin(kR - \varphi_m) = 0,$$

$$\varphi_m = \pi\{m + (r_0^2 + 1)/2\}/2, \tag{13}$$

instead of Eq. (12c).

Postponing till later the proper wave function normalization we assume that $B = \cos\Phi$ and $C = \sin\Phi$ and rewrite the above equation as

$$\cos(kR - \varphi_m - \Phi) = 0. \tag{14}$$

This equation shows that the eigenvalues of the considered problem are approximately separated by $\Delta k = \pi/R$, and reduce to a continuum spectrum in the limit $R \to \infty$. Constructing some averaged description which is valid when calculating the local density of states, we replace Eq. (12c) by the following one:

$$B^2 + C^2 = 1. \tag{15}$$

Now solving it together with Eqs. (12a) and (12b) we obtain three constants:

$$A = -\frac{2}{\pi r_0} W, \quad B = WQ, \quad C = -WP, \tag{16}$$

with

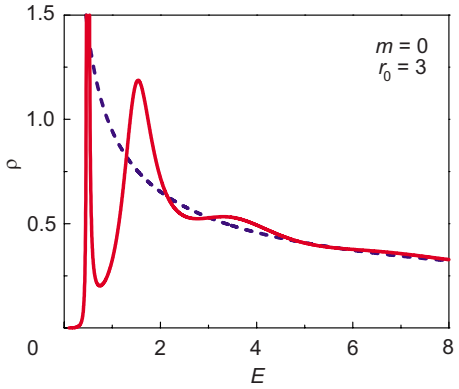

FIG. 3. (Color online) The local density of states for $m=0$ and $r_0=3$ shown by the solid red curve. The same density calculated for a free electron according to Eq. (20) is shown by the blue dashed curve.

$$P = J_{\nu} f_r - J_{\nu,r} f, \tag{17a}$$

$$Q = Y_{\nu} f_r - Y_{\nu,r} f, \tag{17b}$$

$$W = (P^2 + Q^2)^{-1/2}. \tag{17c}$$

The obtained constants enable us to calculate integral (10).

In order to convert the above integral into the local density of states we have to multiply it by two additional constants. One of them is the wave function normalization factor, N, which can be estimated calculating the integral of the squared wave function in the limit of large radius R. The replacement of the Bessel functions by their asymptotic immediately leads to $N = k/2R$. The second one is a consequence of the replacement of the summation over the discrete eigenvalues by the integration over energy, which is given by the factor $R/\pi k$. Together they give $1/2\pi$, which results into definition of the local density of states

$$\rho(E) = \frac{1}{2\pi} \mathcal{I}(E). \tag{18}$$

C. Numerical results

We solved numerically Eq. (17). Inserting the obtained results into Eq. (16), and later in Eqs. (7) and (8), we obtained the wave function which enabled us to calculate integral (10), and finally local density of states (18).

A typical result for the local density of states as a function of electron energy is shown in Fig. 3. We clearly see peaks close to the energies of Landau levels (9) calculated for the case of a homogeneous magnetic field. These peaks are broadened indicating that they are not really bound states in the magnetic dot. The broadening is larger for higher energy peaks.

The next thing which also is seen in Fig. 3 is a decreasing background with energy. This background is due to the states of the free electron in the absence of the magnetic dot. To justify this statement we made the same averaging (over circle of radius r_0) with the same Gaussian aperture function

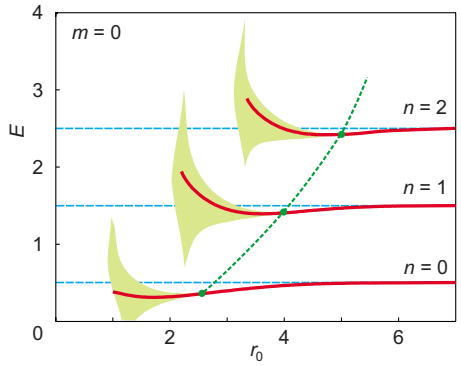

FIG. 4. (Color online) Quasibound states with orbital momentum $m=0$. The energies of these states are given by red solid curves and the widths (i.e., the inverse of the lifetime) by shadowed regions. The Landau levels are indicated by blue dashed lines.

(11) of the radial component of the free electron wave function (when there is no magnetic dot). This function reads

$$\psi_{\text{free}}(r) = J_m(kr) \tag{19}$$

and is valid in the whole 2D plane. Inserting this function into integral (10) and later in Eq. (18) and using tables of integrals[20] we obtain the local density of states for a free electron

$$\rho_{\text{free}}(E) = \frac{r_0^2}{2} e^{-E/b} I_m(E/b), \tag{20}$$

where $I_m(x)$ stands for the modified Bessel function of the first kind. This local density of free electron in the case of $m=0$ is shown in the same Fig. 3 by the blue dashed curve. Comparing these two curves we clearly see how increasing the electron energy we reduce the influence of the magnetic dot on the electron behavior, and the local density of states converts itself gradually into the free electron one.

We fitted the peaks in the density of states by Lorentzian functions $a_n\gamma_n/\{(E-E_n)^2+\gamma_n^2\}$ defining three parameters for any of them: the position E_n, its broadening γ_n, and the amplitude a_n. Two of them (the position and broadening) are shown in Figs. 4 and 5 for different orbital momenta as functions of the radius of the dot r_0. The positions of the quasi-

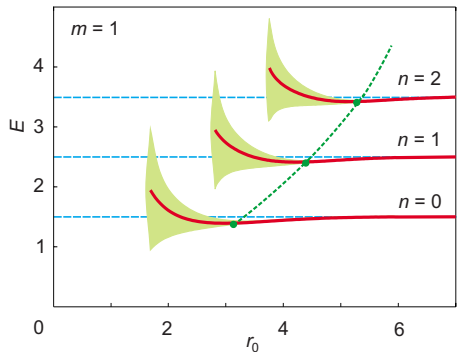

FIG. 5. (Color online) The same as Fig. 4 but now for $m=1$.

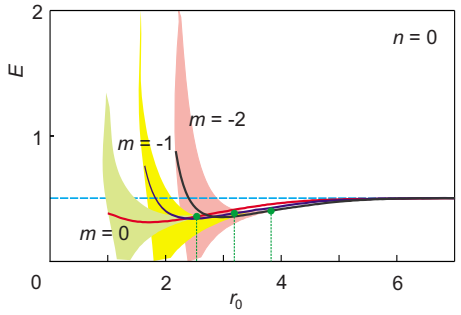

FIG. 6. (Color online) The lowest quasibound state with $n=0$ and different negative m values. The vertical dotted green lines are the analog of the dotted curve in Figs. 4 and 5, separating the weakly broadened states from those with small lifetime.

bound states E_n are shown by the red solid curves while the broadening of the peaks is indicated by the shadowed areas limited by the $E_n \pm \gamma_n$ curves.

Notice that the levels to the right of the green dotted curve are extremely narrow and their position coincides with Landau levels (9) shown by the blue dashed horizontal lines. In fact this means that almost all electron wave function is located in the magnetic dot (using the classical description language we may say that the electron rotates along the Larmor circle inside the dot) and it does not touch the border of the magnetic dot. When the dot radius r_0 becomes smaller the Larmor circle touches the dot border and tunneling of the electron outside the dot starts which broadens the level. The partial penetration of the wave function outside the dot leads to a lowering of the quasibound state energy as well. The raising of this energy for small r_0 values is caused by the large asymmetry of the peak where actually the approximate replacement of the peak by a Lorentzian-type function is no longer valid. This picture is more or less the same for all positive m values (compare Figs. 4 and 5). The difference is that for larger m values the levels start at higher energies, which is in agreement with the expression for Landau levels (9).

The picture for negative m values is different as shown in Fig. 6. All of them belong to the same Landau level energy which is an expression of the degeneracy of the Landau level. We see that with decreasing radius of the dot r_0 the levels with different m disappear step by step; the ones with smaller absolute m values disappear later. This is in agreement with the fact that the larger the $|m|$ value the larger the radius of the electron trajectory, and the electron wave function is closer to the dot edge.

The increase in the peak broadening at small r_0 values is so steep that it is worth to divide all the peaks into two classes as shown in the above figures by the green dotted curves. The levels on the left side of these curves belong to essentially broadened quasibound states, while those on the right side from the experimental point of view can hardly be distinguished from the real bound states.

One can rudely estimate the position of this dividing curve comparing the approximate dimensions of the electron wave function calculated in the case of a homogeneous magnetic field [which actually coincides with function (7)] with the magnetic dot radius r_0. A more accurate estimation can

be obtained solving the stationary Schrödinger equation for complex energy eigenvalues as was described in Ref. 6. We draw these dividing curves in Figs. 4–6 using this technique which is sketched in Sec. II D.

D. Complex energy technique

According to Ref. 6 the lifetime of the quasibound state or the trapping time of the electron in the quantum dot can be estimated solving the time-independent Schrödinger equation and applying boundary conditions of the outgoing waves at the sharp dot border. In our case this technique reduces to connecting the wave function (7) defined in the dot with the outgoing electron wave function outside it, which is given by the first kind Hankel function

$$\psi_{\text{out}}(r) = H_\nu^{(1)}(kr) = J_\nu(kr) + iY_\nu(kr) \tag{21}$$

with

$$\nu = m + r_0^2/2. \tag{22}$$

Applying the boundary conditions for these wave functions and their derivatives we obtain the following equation:

$$f_r(r_0)H(kr_0) - f(r)H_r(kr_0) = 0, \tag{23}$$

where for the sake of simplicity we omitted the indexes of the Hankel functions. The indexes which are only left indicates the derivative over the coordinate r. This equation has to be solved for a complex energy (or complex k); the imaginary part of the energy gives the inverse of the lifetime.

For finding the dotted curves in Figs. 4–6 separating the quasibound and nearly bound states it is enough to solve the above equation by means of a perturbation expansion in terms of the momentum difference $\Delta k = k - k_0$ where $k_0 = \sqrt{2E_{n,m}}$ with energy $E_{n,m}$ of the unperturbed Landau level. Limiting ourselves to first order in Δk we arrive at the following expression:

$$\Delta k = \frac{H_r f - H f_r}{H f_{r,k} + H_k f_r - f H_{r,k} - H_r f_k}. \tag{24}$$

All functions and their derivatives over r and k have to be calculated at $r = r_0$ and $k = k_0$.

Now introducing the energy deviation from the Landau level energy

$$\Delta E = E - E_{n,m} \approx k_0 \Delta k, \tag{25}$$

taking its imaginary part and equating it to 10^{-2} (it is expected that a smaller broadening can hardly be revealed experimentally) we obtained the points connected by the green dotted curve in Figs. 4–6 separating the quasibound states from nearly bound states.

III. DIRAC ELECTRON IN GRAPHENE

Now we repeat the above calculation for the magnetic dot applying it to the case of a Dirac electron in graphene, where the low-energy quasiparticles (electrons and holes) are described by the following dimensionless Dirac-type Hamiltonian:

$$H = \boldsymbol{\sigma}(-i\nabla + \mathbf{A}). \tag{26}$$

Here, $\boldsymbol{\sigma} = \{\sigma_x, \sigma_y\}$ stands for the 2×2 Pauli matrices. The units are based on the magnetic-field strength B_0 and they are the same as in previous section, except the unit of energy which now is $v_F \hbar / l_B$ with the Fermi velocity $v_F = 10^8$ cm s^{-1}. In the case of a 1 T magnetic field this energy unit is 2.6 meV. The vector potential is given by Eq. (3).

A. Solution of eigenvalue problem

The approach is based on the same stationary Schrödinger Eq. (1) but now with the matrix Hamiltonian (26), which results into a set of two differential equations. Assuming the wave function of the following form:

$$\Psi = e^{im\varphi} \begin{pmatrix} a(r) \\ ie^{i\varphi} b(r) \end{pmatrix}, \tag{27}$$

we arrive at a set of two equations for the radial wave function components

$$\left\{ \frac{d}{dr} + A(r) + \frac{m+1}{r} \right\} b = Ea, \tag{28a}$$

$$-\left\{ \frac{d}{dr} - A(r) - \frac{m}{r} \right\} a = Eb, \tag{28b}$$

which has to be solved in the two regions (I in the dot, and II—outside it). We require the continuity of the obtained components at the dot border r_0

$$a_{\text{I}}(r_0) = a_{\text{II}}(r_0), \quad b_{\text{I}}(r_0) = b_{\text{II}}(r_0). \tag{29}$$

Instead of solving these first-order differential equations it is more convenient to convert them into second-order differential equations for a single component, say for component b,

$$\left\{ \frac{1}{r}\frac{d}{dr} r \frac{d}{dr} - \frac{(m+1)^2}{r^2} - \frac{r^2}{4} + [E^2 - m] \right\} b_{\text{I}} = 0, \tag{30a}$$

$$\left\{ \frac{1}{r}\frac{d}{dr} r \frac{d}{dr} + \left[E^2 - \frac{(m + 1 + r_0^2/2)^2}{r^2} \right] \right\} b_{\text{II}} = 0. \tag{30b}$$

In contrast to the electrical quantum dot case, which was considered in Ref. 5, now the effective potential in Eq. (28) is a continuous function at the dot border. For this reason boundary conditions (29) are equivalent to

$$b_{\text{I}}(r_0) = b_{\text{II}}(r_0), \quad b_{\text{I},r}(r_0) = b_{\text{II},r}(r_0). \tag{31}$$

These boundary conditions are identical to those for the previous Schrödinger electron case (12). It enables us to use the full analogy with the previous case. Taking this analogy into account we have for the solution in the two regions,

$$b_{\text{I}}(r) = Af(r) = Ar^{|m+1|} e^{-r^2/4} M(a_0 | c_0 | r^2/2), \tag{32a}$$

$$b_{\text{II}}(r) = BJ_\nu(kr) + CY_\nu(kr), \tag{32b}$$

where $k = |E|$, $a_0 = (|m+1| + m + 1 - E^2)/2$, $\nu = m + 1 + r_0^2/2$, and $c_0 = |m+1| + 1$. The expressions for the other wave function

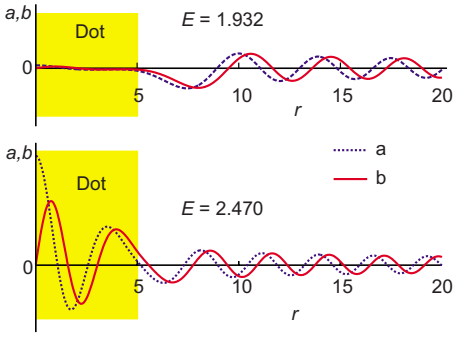

FIG. 7. (Color online) The wave function components: a—dashed blue curve, and b—red solid curve, for $m=0$, dot radius $r_0=5$ and two energy values: $E=1.932$—upper plot, $E=2.470$—lower plot.

component $a(r)$ follow directly from Eq. (28a):

$$a_{\mathrm{I}}(r) = \frac{A}{E} r^{|m+1|} e^{-r^2/4} \times \left\{ \frac{d}{dr} + \frac{|m+1|+m+1}{r} \right\} M(a_0|c_0|r^2/2), \tag{33a}$$

$$a_{\mathrm{II}}(r) = BJ_{\nu-1}(kr) + CY_{\nu-1}(kr). \tag{33b}$$

The wave function components obtained in the above way are illustrated in Fig. 7 for two different values of the energy.

We see the same tendency. When the energy is close to the Landau level energy of the Dirac electron in a homogeneous magnetic field,

$$E_{n,m} = \pm \sqrt{2n + |m+1| + m + 1}, \tag{34}$$

(see the lower plot of Fig. 7 where the energy is close to the Landau level with $m=0$, $n=2$) we see a clear accumulation of the wave function components in the dot, which indicates a quasibound state.

B. Local density of states

Developing further the analogy of Eq. (30) with the considered previously case we calculated the local density of states using Eqs. (17), (16), and (10). Because we have now a wave function with two components, Eq. (10) is modified into

$$\mathcal{I}(E) = 2\pi \int_0^\infty rdrF(r)\{|a(r)|^2 + |b(r)|^2\}. \tag{35}$$

Now the normalization factor is $N=k/4R$ (due to the two wave function components), and the factor responsible for the change of the summation over discrete eigenvalues into an integral over the electron energy is R/π. Thus, the local density of states in the case of a Dirac electron becomes

$$\rho(E) = \frac{|E|}{2} \int_0^\infty rdrf(r)\{|a(r)|^2 + |b(r)|^2\}. \tag{36}$$

In the case of free Dirac electrons (when there is no magnetic dot) the wave function components read

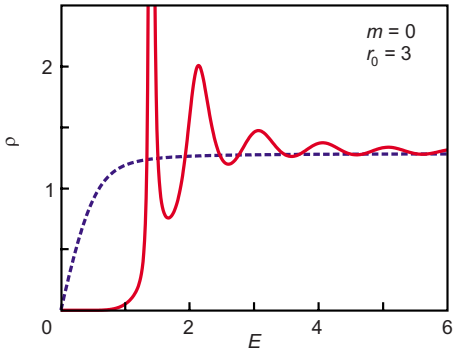

FIG. 8. (Color online) The local density of states for a Dirac electron in the magnetic dot for $m=0$ and $r_0=3$ shown by red solid curve. The dashed blue curve is the free electron density of states.

$$a_{\mathrm{free}} = J_m(kr), \quad b_{\mathrm{free}} = J_{m+1}(kr), \tag{37}$$

which leads to the following expression of the local density of states for a free electron:

$$\rho_{\mathrm{free}}(E) = \frac{|E|r_0^2}{4} e^{-E^2/2b}\{I_m(E^2/2b) + I_{m+1}(E^2/2b)\}. \tag{38}$$

C. Numerical results

The typical local density of states calculated for $m=0$ and $r_0=3$ is shown in Fig. 8 for positive energies. Two differences with respect to standard electrons can clearly be noticed. First, in the case of the Dirac electron the spectrum is symmetric with respect to energy inversion ($E \to -E$) due to the equivalence of electrons and holes. Thus the plot in Fig. 8 has to be supplemented by the same curves for negative energies. Second, comparing the density of states for Dirac electron with the same curve for the Schrödinger one (see Fig. 3) we see that there are more peaks. This can be explained by the more dense Landau level spectrum in the case of Dirac electrons (34) for the large quantum number values as compared with these for the previous case (9).

As before we fit the peaks by Lorentz-type curves, which leads to the broadened levels displayed in Figs. 9 and 10. We see that the levels with $m=-1$ start at lowest energies, which is just the consequence of chosen definition of radial wave function components (27).

The green dotted curves divide the region of broadened quasibound states from the region where the states have a very small broadening. These curves were obtained in the same way as it was done in Sec. II D for the case of Schrödinger electron, namely, applying the complex energy eigenvalue technique. In the case of the Dirac electron it leads to the following imaginary energy part:

$$\Delta = \frac{H_{\nu-1}b - H_\nu a}{H_{nu}a_r + H_{\nu,r}a - H_{\nu-1}b_r - H_{\nu-1,r}b}. \tag{39}$$

The above-mentioned dotted green line corresponds to $\delta=3 \times 10^{-3}$. Note we chose it three times smaller than in Figs. 4–6, which causes us to conclude that between the local density of states technique and complex energy eigenvalue

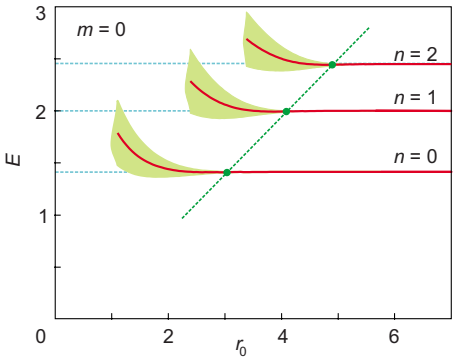

FIG. 9. (Color online) Quasibound states with orbital momentum $m=0$ for the Dirac electron in the magnetic dot. The energy of these states is given by red solid curves and its width (i.e., the inverse of the lifetime) by the shadowed regions. The Landau levels are indicated by blue dashed lines.

method one can expect only qualitative agreement.

There is one more interesting point—the zero-energy state which is shown in Fig. 10 by thick red line along the x axis. Its behavior differs essentially from all other states. That is why it needs some special attention which is presented in Sec. III D.

D. Zero-energy state

Now we check whether the Dirac electron has a zero-energy state in the magnetic dot. In this case instead of Eq. (28) we have to solve the following two equations for the radial components of the electron wave function:

$$\left\{\frac{d}{dr}+A(r)+\frac{m+1}{r}\right\}b=0, \tag{40a}$$

$$\left\{\frac{d}{dr}-A(r)-\frac{m}{r}\right\}a=0. \tag{40b}$$

These are uncoupled differential equations of the first order, and their solution can be found by a straightforward integration. The solution has the following asymptotic behavior:

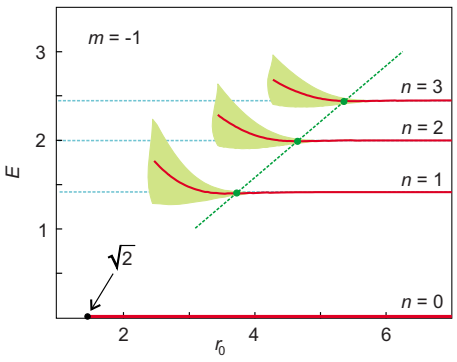

FIG. 10. (Color online) The same as Fig. 4 but now for $m=-1$.

$$\ln a(r)=\int dr\left\{A(r)+\frac{m}{r}\right\}\sim\begin{cases} m\ln r+r^2/4, & r\to 0\\ (m+r_0^2/2)\ln r, & r\to\infty,\end{cases} \tag{41}$$

and

$$\ln b(r)=-\int dr\left\{A(r)+\frac{m+1}{r}\right\}\sim\begin{cases}-(m+1)\ln r-r^2/4, & r\to 0\\ -(m+1+r_0^2/2)\ln r, & r\to\infty,\end{cases} \tag{42}$$

or

$$a(r)\sim\times\begin{cases} r^m\exp(r^2/4), & r\to 0\\ r^{m+r_0^2/2}, & r\to\infty,\end{cases} \tag{43}$$

and

$$b(r)\sim\begin{cases} r^{-m-1}\exp(-r^2/4), & r\to 0\\ r^{-(m+1+r_0^2/2)}, & r\to\infty.\end{cases} \tag{44}$$

In order to have the wave function with finite norm two boundary conditions have to be satisfied. First, the function should behave like r^α $(\alpha\geq 0)$ when $r\to 0$, and second, it should behave like $r^{-\alpha}$ $(\alpha\leq -1)$ when $r\to\infty$.

For the a component the above conditions reduce to the requirements $m\geq 0$ and $m+r_0^2/2\leq -1$, which cannot be satisfied simultaneously. Consequently, we have to assume that $a=0$.

In the case of component b the conditions read

$$-r_0^2/2\leq m\leq -1, \tag{45}$$

from which it follows that if $r_0^2/2\geq 1$ there are always some negative m values for which a zero-energy state exists. When the radius of the dot decreases, this interval becomes smaller, and the zero-energy states vanish one by one. Finally, at $r_0^2/2<1$ all of them disappear.

Such essential difference between the bound zero-energy level and all other quasibound levels is caused by the fact that the wave function of the state with zero energy is real. Consequently, the electron in this state has no velocity, and as a result there is no tunneling of this electron outside the dot. Unfortunately, the absence of any nonzero electron velocity makes it impossible to reveal this state in transport measurements, but maybe it can reveal itself through the statistic properties of the magnetic dot.

IV. CONCLUSIONS

We considered the eigenvalue problem of a model quantum magnetic dot where the homogeneous magnetic field perpendicular to the 2D electron motion plane is created only in a finite region—in a circle of radius r_0. We showed that such a magnetic field fails to confine electrons both for the standard parabolic dispersion law or the ultrarelativistic linear dispersion law for Dirac electrons in graphene. Although in such a magnetic dot no confined states are found, quasibound sates with a finite lifetime are present.

An analysis of the quasibound states for the Schrödinger and Dirac electron was performed by means of the local density of states, and the position and width of the resonance peaks (the analogs of the quasistationary states) on the dot radius (or the strength of the magnetic field) were calculated. The broadening of these peaks (the inverse lifetime of the quasibound state) is mainly caused by the touching of the quantum dot border by the electron wave function tail. Due to the exponential character of this tail there exists a rather sharp border between broadened quasibound states and those which can be considered as nearly bound ones. This border was found by applying the complex energy eigenvalue method which is shown to be in qualitative agreement with the results obtained from the local density of states technique.

It is shown that the difference of the quasibound states in the magnetic dot between the Schrödinger and Dirac electrons is only in the energies of these states which is a consequence of the different energies of the corresponding Landau levels. There is a single exception: in the case of Dirac electrons there exists a zero-energy bound state for negative values of the angular momentum (the momentum which is opposite to the direction of the classical electron rotation along the Larmor circle). When the dot radius r_0 (or the magnetic-field strength) decreases the degeneracy of this zero-energy level decreases skippingly while all other quasibound states disappear smoothly via their broadening.

ACKNOWLEDGMENTS

This work was supported by the Flemish Science Foundation (Grant No. FW0-Vl), CNPq (Brazil science funding agency), and the Belgian Science Policy (IAP).

*mrmphys@gmail.com
†amatulis@takas.lt
‡francois.peeters@ua.ac.be

[1] K. S. Novoselov, A. K. Geim, S. V. Morozov, D. Jiang, M. I. Katsnelson, I. V. Grigorieva, S. V. Dubonos, and A. A. Firsov, Nature (London) **438**, 197 (2005).
[2] Y. Zhang, Y. W. Tan, H. L. Stormer, and P. Kim, Nature (London) **438**, 201 (2005).
[3] M. I. Katsnelson, K. S. Novoselov, and A. K. Geim, Nat. Phys. **2**, 620 (2006).
[4] Hong-Yi Chen, V. Apalkov, and T. Chakraborty, Phys. Rev. Lett. **98**, 186803 (2007).
[5] A. Matulis and F. M. Peeters, Phys. Rev. B **75**, 125429 (2007).
[6] P. Hewageegana and V. Apalkov, Phys. Rev. B **77**, 245426 (2008).
[7] F. M. Peeters and A. Matulis, Phys. Rev. B **48**, 15166 (1993).
[8] J. Reijniers, F. M. Peeters, and A. Matulis, Phys. Rev. B **64**, 245314 (2001).
[9] J. Reijniers, F. M. Peeters, and A. Matulis, Phys. Rev. B **59**, 2817 (1999).
[10] M. Ramezani Masir, P. Vasilopoulos, A. Matulis, and F. M. Peeters, Phys. Rev. B **77**, 235443 (2008).
[11] A. De Martino, L. Dell' Anna, and R. Egger, Phys. Rev. Lett. **98**, 066802 (2007); Solid State Commun. **144**, 547 (2007).
[12] S. Park and H. S. Sim, Phys. Rev. B **77**, 075433 (2008).
[13] L. Oroszlany, P. Rakyta, A. Kormanyos, C. J. Lambert, and J. Cserti, Phys. Rev. B **77**, 081403(R) (2008).
[14] T. K. Ghosh, A. De Martino, W. Häusler, L. Dell'Anna, and R. Egger, Phys. Rev. B **77**, 081404(R) (2008).
[15] F. Zhai and K. Chang, Phys. Rev. B **77**, 113409 (2008).
[16] M. Tahir and K. Sabeeh, Phys. Rev. B **77**, 195421 (2008).
[17] Hengyi Xu, T. Heinzel, M. Evaldsson, and I. V. Zozoulenko, Phys. Rev. B **77**, 245401 (2008).
[18] S. J. Lee, S. Souma, G. Ihm, and K. J. Chang, Phys. Rep. **394**, 1 (2004).
[19] N. Malkova, I. Gomez, and F. Dominguez-Adame, Phys. Rev. B **63**, 035317 (2001); S. M. Badalyan and F. M. Peeters, *ibid.* **64**, 155303 (2001); J. M. Pereira, Jr., F. M. Peeters, and P. Vasilopoulos, *ibid.* **75**, 125433 (2007).
[20] I. S. Gradshteyn and I. M. Ryzhik, *Tables of Integrals, Series, and Products* (Academic Press, New York, 2000), p. 699.